

Abrupt permafrost thaw triggers activity of copiotrophs and microbiome predators

Maria Scheel^{1,2,*}, Athanasios Zervas¹, Ruud Rijkers^{3,4}, Alexander T. Tveit⁵, Flemming Ekelund^{1,6}, Francisco Campuzano Jiménez¹, Torben R. Christensen^{2,7}, Carsten S. Jacobsen¹

¹Department of Environmental Science, Aarhus University, Roskilde 4000, Denmark

²Department of Ecoscience, Aarhus University, Roskilde 4000, Denmark

³Department of Ecological Science, Vrije Universiteit Amsterdam, 1081 HV Amsterdam, The Netherlands

⁴Department of Environmental Science, Stockholm University, SE-106 91 Stockholm, Sweden

⁵Department of Arctic and Marine Biology, University of Tromsø, Tromsø 9019, Norway

⁶Department of Biology, Copenhagen University, DK-2200 Copenhagen, Denmark

⁷Water, Energy and Environmental Engineering Research Unit, University of Oulu, FI-90014 Oulu, Finland

*Corresponding author. Department of Environmental Science, Aarhus University, Roskilde 4000, Denmark. Tel: +31 618 798369; E-mail: maria.scheel@envs.au.dk

Editor: [Dirk Wagner]

Abstract

Permafrost soils store a substantial part of the global soil carbon and nitrogen. However, global warming causes abrupt erosion and gradual thaw, which make these stocks vulnerable to microbial decomposition into greenhouse gases. Here, we investigated the microbial response to abrupt *in situ* permafrost thaw. We sequenced the total RNA of a 1 m deep soil core consisting of up to 26 500-year-old permafrost material from an active abrupt erosion site. We analysed the microbial community in the active layer soil, the recently thawed, and the intact permafrost, and found maximum RNA:DNA ratios in recently thawed permafrost indicating a high microbial activity. In thawed permafrost, potentially copiotrophic Burkholderiales and Sphingobacteriales, but also microbiome predators dominated the community. Overall, both thaw-dependent and long-term soil properties significantly correlated with changes in community composition, as did microbiome predator abundance. Bacterial predators were dominated in shallower depths by Myxococcota, while protozoa, especially Cercozoa and Ciliophora, almost tripled in relative abundance in thawed layers. Our findings highlight the ecological importance of a diverse interkingdom and active microbial community highly abundant in abruptly thawing permafrost, as well as predation as potential biological control mechanism.

Keywords: abrupt erosion; copiotrophic; permafrost; protozoa; transcriptomics

Introduction

Permafrost soils are among the most vulnerable ecosystems of the globe, both in terms of biodiversity and potential degradation in response to global warming (Abbott et al. 2022, IPCC 2021). Permafrost is found in historically cold regions and remains frozen for at least 2 consecutive years. It consists of a seasonally thawed active layer and permafrost below, often remaining frozen for millennia. These conditions selected for a unique but still elusive microbial communities under constant freezing conditions (Jansson and Tas 2014). Intact permafrost—due to slow microbial at long-term stable freezing temperatures—stores 1100–1500 Pg C, over half of all global soil carbon (C) (Tarnocai et al. 2009, Hugelius et al. 2014), as highly recalcitrant organic matter (Parmentier et al. 2017). As ambient temperatures in the Arctic increase up to four times faster than the global average (Rantanen et al. 2022), active layers gradually thaw deeper into former permafrost (AMAP 2021). In the long term, this enables a deeper rooting vegetation and potential microbial remineralisation of permafrost carbon (Schuur and Mack 2018). Additionally, warming causes ground ice to melt and soils to collapse abruptly, modelled to affect up to half of all permafrost carbon by 2100 (Turetsky et al. 2020).

In ancient microaggregates and brine channels, permafrost harbours resistant taxa that exhibit slow growth rates, higher

metabolic versatility, and an ability to perform syntrophy (Allison and Martiny 2008, Shade et al. 2012), often functionally constrained due to environmental limitations and slow reproduction rates (Monteux et al. 2020). The overlaying thawed soils selected for highly resilient taxa with high growth rates, as temperature seasonally fluctuates (Allison and Martiny 2008, Bardgett and Caruso 2020). Upon thaw, permafrost soil communities, then can become functionally redundant (Nannipieri et al. 2017), both during *in situ* (Monteux et al. 2018) and experimental thaw (Monteux et al. 2020). Thaw-induced perturbation of the ground can cause migrations of microbial taxa from the original active layer towards deeper soils, called coalescence. This can be induced through rapid population growth of copiotrophic taxa and can increase carbon and nitrogen (N) release from thawed permafrost soil (Monteux et al. 2020). These microbial responses to thaw could stem from the revival of former resting stages, such as cysts and endospores (Lennon and Jones 2011), which upon suitable thermal and moisture conditions can lead to locally increased microbial activity.

While so far not described in thawing permafrost soils, the complexity of trophic relations plays a key role in temperate soil carbon mineralisation (Bardgett and van der Putten 2014). Eukaryotes and their importance in permafrost are particularly under-

Received 1 March 2023; revised 31 August 2023; accepted 4 October 2023

© The Author(s) 2023. Published by Oxford University Press on behalf of FEMS. This is an Open Access article distributed under the terms of the Creative Commons Attribution-NonCommercial License (<https://creativecommons.org/licenses/by-nc/4.0/>), which permits non-commercial re-use, distribution, and reproduction in any medium, provided the original work is properly cited. For commercial re-use, please contact journals.permissions@oup.com

studied due to biases and difficulties related to the use of gene-specific primers (Harder et al. 2016), but the use of total RNA sequencing enables a less biased understanding of the putatively active total community. Particularly, the predation on bacteria can act as control and driver of the soil microbiome (Thakur and Geisen 2019, Geisen et al. 2021). Organisms feeding on bacteria, called bacterivores, include predatory eukaryotes, such as protozoa (*sensu* single cell predatory protists; Geisen et al. 2018), nematodes, rotifers, and tardigrades (Coleman and Wall 2015), as well as bacterial taxa, such as the myxobacterial phyla Myxococcota and Bdellovibrionota. Moreover, the selective removal of bacterial cells by predators controls both the bacterial turnover and community composition (Trap et al. 2016). Lysis of prey cells and incomplete mineralisation of organic C and N by protozoa enhance the recycling and distribution of nutrients (Bonkowski 2004). Although microbial predator presence, such as Myxococcota, was documented before in permafrost (Malard and Pearce 2018, Schostag et al. 2019, Scheel et al. 2022), their relevance in Arctic soils is still elusive.

In this study, we investigated the whole active microbial community of recently thawed ancient permafrost and tested how strongly biotic or abiotic factors impact the microbial community in different stages of thaw. Due to their shorter doubling time, we furthermore hypothesised that the freshly thawed soils support higher abundances of copiotrophic taxa. We then discuss their potential origin from the active layer or reactivated permafrost resting stages as well as how their biomass could support a potential bacterivore cascade. These insights can help us understand the spatiotemporal and trophic dynamics of permafrost microbial ecology and estimate the ecological response of gradual and rapid erosion as a potential key driver of both permafrost carbon vulnerability.

Materials and methods

Soil sampling

Sampling took place in 2020 in Zackenberg valley, NE Greenland (74°30'N 20°30'W, Fig. 1A–B). This wide lowland valley is dominated by continuous permafrost and a vegetation of wet hummocky fens, low shrub, and graminoids (Elberling et al. 2008). Average temperatures varied between -2°C in summer and -14°C in winter between 1997 and 2006 (Christiansen et al. 2008). The active layer seasonally thaws between 40 cm and 2 m deep, but an increase of 0.77 cm per year when including data from 1995 to 2020 (Westermann et al. 2015, Westergaard-Nielsen et al. 2018).

The permafrost soil surface collapsed abruptly in 2018 as a formerly described recent, thermal erosion gully developed in the vicinity of the Zackenberg Research Station (Christensen et al. 2020, Scheller et al. 2021, Scheel et al. 2022). Below the active layer (AL) at 40 cm depth, an ice lens had melted in 2019, creating a first transition zone depth until 70 cm depth (TZ1). In 2020, thaw reached until 90 cm depth in 2020 (TZ2), while below 90 cm depth intact permafrost (PF) persisted (Fig. 1C–D). In 2020, three replicate soil samples were taken aseptically per 10 cm intervals until a depth of 1 m, resulting in 30 samples. Due to different RNA stability at varying freezing temperatures (Schostag et al. 2020) and laboratory limitations in the sampling station, the samples were stored at -20°C until transported frozen to Denmark, where they were stored at -80°C .

Physicochemical soil analysis

Physical soil properties were determined in technical triplicate as described in Scheel et al. (2022) from thawed 10-cm soil horizon

samples until 100 cm depth. First after air-drying at 70°C for 48 h, followed by burning at 450°C for 2 h, the samples were weighed to determine the loss of relative weight-based soil water (H_2O) and organic carbon (SOM; Wilke 2005). The pH was measured after adding 50 ml of 1 M KCl to 10 ml of air-dried soil samples with a Mettler Toledo FiveEasy PlusTM pH Meter (Mettler Toledo GmbH, Gießen, Germany).

Radiocarbon dating was performed per 10-cm horizon by sifting thawed soil with a 0.5-mm sieve retaining macro plant residues and excluding roots. Per depth, triplicates were pooled, treated with HCl and NaOH, graphitised, and ^{14}C isotope activity was measured using an accelerator mass spectrometer (Radiocarbon Dating Laboratory, Lund University, Lund, Sweden). The resulting age was calibrated with IntCal13 (Reimer et al. 2016) to ^{14}C years in BP (before present = AD 1950) and the Levin post-Bomb calibration (Levin and Kromer 2016) for results in fM (fraction modern) after 1963.

Nucleic acid co-extraction, library preparation, and sequencing

Deep-frozen samples were homogenised in antiseptic mortars. Then we co-extracted the total RNA and DNA of the biological replicates on up to 0.35 g frozen soil sample with the NucleoBond RNA Soil Mini kit (Macherey-Nagel GmbH & Co. KG Dueren, Germany) according to the manufacturer's protocol. We used G2 DNA/RNA Enhancer infused 1, 4 mm beads (Ampliqon, Odense, Denmark) instead of the ones provided with the kit. To remove potential DNA, the RNA extracts were treated with the DNase Max Kit (QIAGEN), following the manufacturer's protocol. Both the removal of DNA and final RNA concentrations were evaluated and confirmed using a Qubit[®] 4 Fluorometer (Thermo Fisher Scientific, Life Technologies, Roskilde, Denmark). We quality-assessed the final extracts with a TapeStation 4150 (Agilent Technologies, Santa Clara, CA, USA) using a high-sensitivity assay. Resulting RNA integrity numbers (RIN) were low (1.0 ± 0.6 , Supplementary Table 1) and samples from 80 to 100 cm depth had RNA concentrations below detection limit. Nucleic acid concentrations were normalised for sample weight and used for extraction ratios of extracted RNA to DNA (RNA:DNA, Table 1). We fragmented the RNA, synthesised cDNA, and processed the cDNA with the NEBNext Ultra II Directional RNA Library Prep Kit and the NEBNext Multiplex Oligos for Illumina (New England BioLabs, Ipswich, MA, USA), following the manufacturer's protocol. The resulting samples were pooled into equimolar metatranscriptome libraries to secure even sequencing coverage. We performed the sequencing in-house (Department of Environmental Science, Aarhus University, Denmark) on an Illumina NextSeq 500 with a v2.5 high-throughput 300 cycles kit (both Illumina, San Diego, CA, USA).

Bioinformatic processing

The 352 Mio. raw paired-end Illumina reads (SRA accession number: PRJNA939404, Table 1) were quality-controlled with TrimGalore (https://www.bioinformatics.babraham.ac.uk/projects/trim_galore/) and filtered by removing adapters and short reads (<60 nt). These sequences were then classified (sorted) into small subunit (SSU) rRNA, large subunit (LSU) rRNA, and non-rRNA sequences by aligning to SILVA 138.1 SSU Ref NR 99 and SILVA 138.1 LSU Ref NR 99 using SortMeRNA (Kopylova et al. 2012). The SSU reads were assembled into full-length SSU rRNA contigs with MetaRib (Xue et al. 2020). These rRNA contigs were taxonomically classified as described by Anwar and colleagues (Anwar et al. 2019), using CREST4 (Lanzen et al. 2012) against the

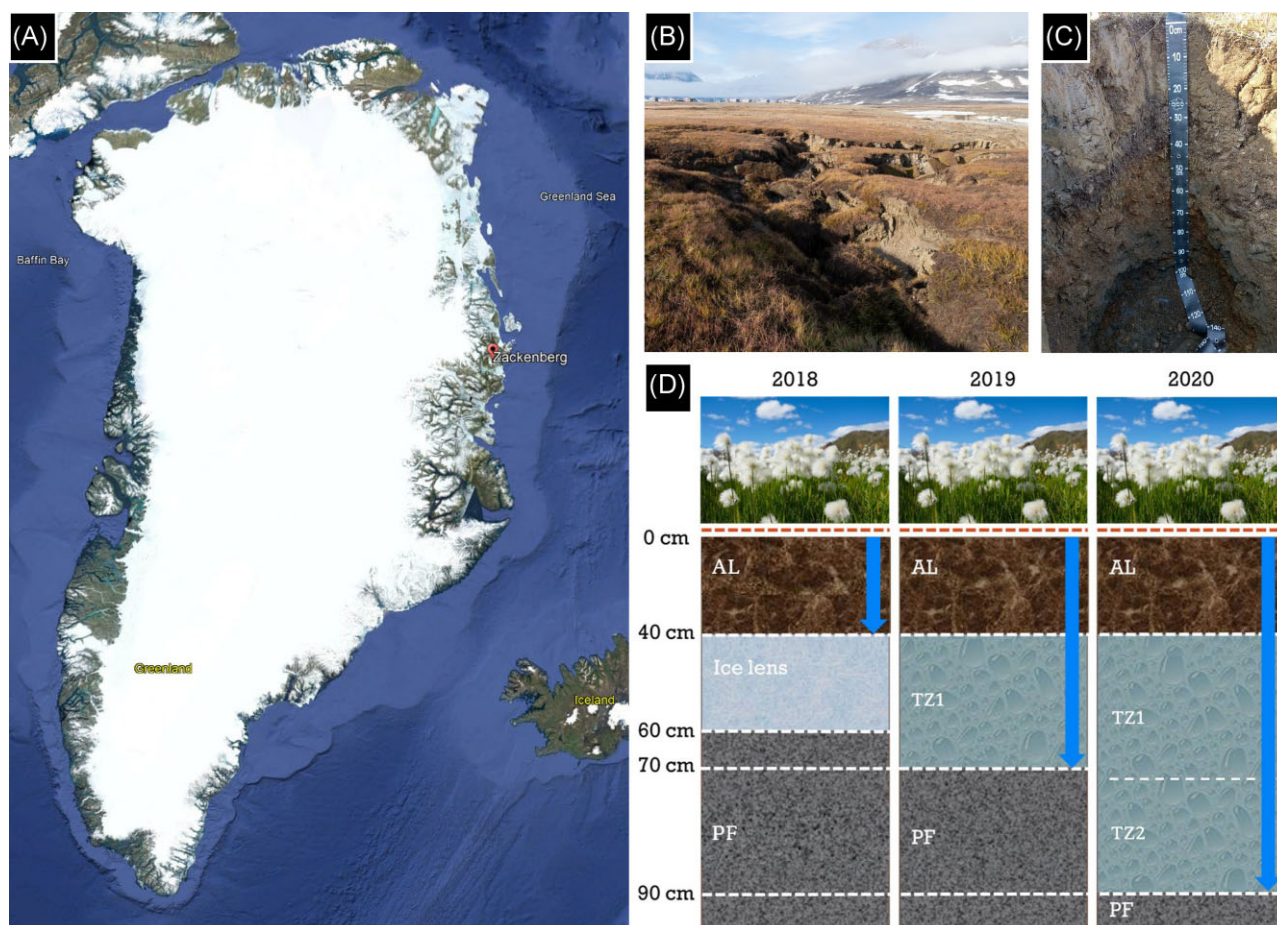


Figure 1. (A) Sampling site Zackenberg in Northeast Greenland, credit: Google Earth. (B) Sampling site in 2018 after initial permafrost collapse. (C) Soil profile from the surface until still frozen depth at 90 cm during sampling in 2020. (D) Scheme of abrupt permafrost thaw (indicated with blue arrows), depicting the soil profile until the permafrost (PF) layer at 90–100 cm depth from the moment of collapse in 2018 with visible ice lens below long-term active layer (AL) to the formation of transition zones (TZ = thawed permafrost).

Table 1. Soil properties include ^{14}C (radiocarbon) dating results (* = fM; **BP), relative weight-based soil moisture (H_2O), relative weight-based soil organic matter content (SOM), pH and layer, as defined by thawing processes as active layer (AL); deepest thaw in 2019: transition zone 1 (TZ1) and 2020: TZ2; and permafrost (PF).

Depth [cm]	^{14}C [*fM]		H_2O [%]	SOM [%]	pH	Layer	DNA ng/gDW	RNA ng/gDW	RNA:DNA	Total reads
	**BP									
0–10	1.04*		28.80 ± 3.38	8.73 ± 1.82	4.22 ± 0.03	AL	835.55 ± 391.99	357.46 ± 171.55	0.46 ± 0.16	$1.25\text{E}+07$
10–20	1.13*		22.52 ± 0.73	5.39 ± 0.83	4.02 ± 0.05		82.65 ± 93.13	72.99 ± 8.38	1.78 ± 1.28	$4.85\text{E}+07$
20–30	1.16*		22.05 ± 3.30	10.19 ± 3.22	4.29 ± 0.01		561.38 ± 571.54	91.19 ± 1.99	0.29 ± 0.19	$2.25\text{E}+07$
30–40	1.2*		26.57 ± 0.83	13.68 ± 0.44	4.25 ± 0.01		186.67 ± 33.49	86.43 ± 23.06	0.49 ± 0.20	$6.07\text{E}+07$
40–50	2635**		7.73 ± 1.58	2.59 ± 0.68	4.63 ± 0.03	TZ1	54.68 ± 60.24	40.66 ± 42.59	0.83 ± 0.91	$2.39\text{E}+07$
50–60	3770**		15.61 ± 6.28	2.93 ± 0.30	4.13 ± 0.02		10.99 ± 9.45	40.51 ± 10.58	9.34 ± 11.03	$7.22\text{E}+07$
60–70	26 500**		8.72 ± 2.53	1.52 ± 0.16	4.86 ± 0.05		8.66 ± 11.41	36.19 ± 4.39	11.98 ± 9.47	$4.90\text{E}+07$
70–80	22 100**		6.35 ± 0.60	1.10 ± 0.24	4.48 ± 0	TZ2	2.11 ± 11.97	17.94 ± 31.07	18.48 ± 32.02	$1.49\text{E}+07$
80–90	26 200**		7.96 ± 0.61	1.00 ± 0.20	4.57 ± 0.01		1.04 ± 1.80	NA	NA	$3.46\text{E}+07$
90–100	26 200**		7.80 ± 0.59	1.04 ± 0.26	4.91 ± 0.01	PF	0.96 ± 1.66	NA	NA	$1.40\text{E}+07$

Extraction and sequencing output included the calculated RNA:DNA ratio based on co-extraction of nucleic acids in ng yield per gram dry weight (gDW). The cumulative sum of clean total RNA sequencing reads per depth. Standard deviations for triplicates per depth are indicated where available (\pm).

SILVA database v.138 (Quast et al. 2013) and PR2 database (Guillou et al. 2013). The resulting annotation was partly outdated and corrected per contig (Supplementary Methods). The rRNA reads were mapped to resulting EMIRGE contigs using BWA (Li and Durbin 2009), resulting in taxonomically annotated rRNA contig abundance across the 30 samples. The automatic pipeline used is available (Campuzano Jiménez 2023).

rRNA processing

The taxonomic sequence abundance was scanned for previously documented protozoan taxa: Amoebozoa, SAR, Euglenozoa, Foraminifera, and Heterolobosa (Geisen et al. 2015) and Endomyxa, Telonemia, Malawimonadidae, and Choanoflagellida. Bacterial predators included Myxococcota (excluding the genus

Sorangium), Bdellovibrionata, *Lysobacter*, *Daptobacter*, and *Vampirococcus* (Petters et al. 2021, adapted according to SILVA v.138 taxonomy). The rRNA relative abundance was calculated and collapsed taxonomically into prokaryotes, eukaryotes, and further into bacterial predators and protozoa.

Statistical analysis and data processing

For statistical analysis, macroeukaryotes were removed from the dataset, to only depict microbial interactions. We performed community analysis with the R software v.4.2.2 in R studio (RStudio Team 2020, R Core Team 2022), using the phyloseq v. 1.42.0 (McMurdie and Holmes 2013) and vegan v. 2.6.4 packages (Oksanen et al. 2022). We excluded the triplicate 1 of 30 (for the depth 0–10 cm) for all downstream analysis, due to significantly low number of reads (360 opposed to an average 12 Mio. reads per triplicate). Shannon (S) alpha diversity was calculated on the total number of rRNA contigs and abundance of sequence reads mapped per sample (Supplementary Table 1). The significance of environmental data (age, pH, SOM, H₂O, and layer) and of bacterial and protozoan predator abundance were tested with the *anova* function (PERMANOVA, 999 permutations) on Bray–Curtis dissimilarities of relative abundance per taxon within the sample to account for different read coverage across samples. For predation effects, we performed the tests on Bray–Curtis dissimilarities of only nonpredatory prokaryotic and eukaryotic communities. We performed consecutive Tukey's HSD *post-hoc* tests to determine significant difference between taxonomic groups with layer and age as explanatory variables. Variance partitioning was performed on PERMANOVA results for thaw-related (layer and H₂O), long-term soil (SOM, pH, age) as well as biotic (bacterial and protozoan predation) parameters. Nonmetric multidimensional scaling (NMDS) plots were ordinated graphically using Bray–Curtis dissimilarities between samples of the subset communities. Potential predator-prey interactions were investigated using the Sparse Inverse Covariance estimation for Ecological Association and Statistical Inference (SPIEC-EASI) analysis (Kurtz et al. 2015) as can be found in the Supplementary Materials.

Results

Physicochemical soil properties

Radiocarbon results differed greatly with depth, indicating three age categories, that were used for downstream statistical analysis. A more recent upper consisted of organic material and silt (AY), a deeper 2635–3770-year-old inorganic silt layer (AM), and the underlying deepest 22100–26500-year-old layer of inorganic sand and gravel (AO; Table 1). Soil moisture was highest in the active layer until 40 cm depth and then stayed rather stable at 6.35%–8.72%, while pH stayed stable throughout between 4.02 and 4.91 (Table 1). Despite low biomass (174.4 ± 334.7 ng/gDW DNA; 47.3 ± 111.7 ng/gDW RNA), extraction of RNA and DNA was successful in all triplicates and RNA:DNA ratios indicated higher values in the transition zones (Supplementary Fig. 1; Supplementary Table 1).

Total rRNA community composition

In total, 5989 full-length rRNA gene contigs were constructed with an average length of 1474 bp. On average, 74.6% of all reads could be annotated as SSU rRNA and 65.5% of the trimmed reads mapped back to the assembled full-length rRNA genes. Of these, 5969 were annotated on domain level, but annotation success decreased above family level (3353 contigs = 56.2% anno-

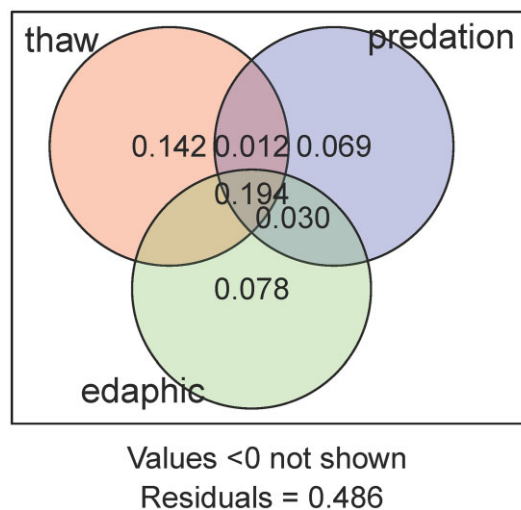


Figure 2. Venn diagram illustrating variance partitioning, which was performed on thaw-related (layer, H₂O), long-term soil (SOM, pH, age) as well as biotic parameters (bacterial and protozoan predator abundance) and their correlation with variance in the overall community composition. Values are given for R² values, based on PERMANOVA results (999 permutations) on Bray–Curtis dissimilarities.

tated, Supplementary Table 1). Overall, 5582 rRNA contigs were assigned as Bacteria (79.6% ± 0.1% of total counts), 374 as Eukarya (14.8% ± 0.2%), and 16 as Archaea (0.1% ± 0.0%). Omnipresent in each sample were 3900 rRNA contigs (65.1% of contigs, 91.7% of all counts). Yet, 2635 rRNA contigs were most abundant in active layer (44.0% of contigs, 26.9% of all counts). Only 573 and 294 rRNA contigs were most abundant specifically in TZ1 and TZ2, compromising only 9.6% and 4.9% of contigs, but 12.2% and 9.6% of all counts, respectively. Further, 245 rRNA contigs were most abundant in permafrost (4.1% of contigs, 6.2% of all counts).

Prokaryotic community composition and distribution with depth

The prokaryotic community was dominated by Proteobacteria (21.8% ± 0.1% of total counts), Actinobacteriota (15.0% ± 0.1% of total counts), Acidobacteriota (8.1% ± 0.0% of total counts), Bacteroidota (6.3% ± 0.1% of total counts), and Myxococcota (6.0% ± 0.1% of total counts; Fig. 3A). Further, 51 bacterial phyla (including 16 Candidate phyla) and 7 archaeal phyla were present. Proteobacteria increased in relative abundance between 50 and 90 cm, the depth of the two thaw layers. This phylum was dominated by the gammaproteobacterial Burkholderiales (14% ± 0.1% of total counts) with maximum abundances at 70 and 90 cm depth, respectively. The abundance of Actinobacteriota decrease with depth, but peaked in permafrost, while Acidobacteriota were most abundant in the active layer. Bacteroidota abundances increased with depth, especially within 70–100 cm, responding to the layers TZ2 and permafrost. Especially, Sphingobacteriales rRNA contigs constituted 3.0% ± 0.2% of all counts and reached maximum abundances at 70–80 cm.

Microeukaryotic permafrost community

Eukaryotes were dominated by Plantae rRNA contigs (7.5% ± 0.6% of total counts). Together with Metazoa (0.5% ± 0.3%), such as Arthropoda and Tardigrada rRNA contigs, macroeukaryotes were removed from further statistical analysis. Fungi were overall present at low relative abundance of 0.6% ± 0.0% of the total

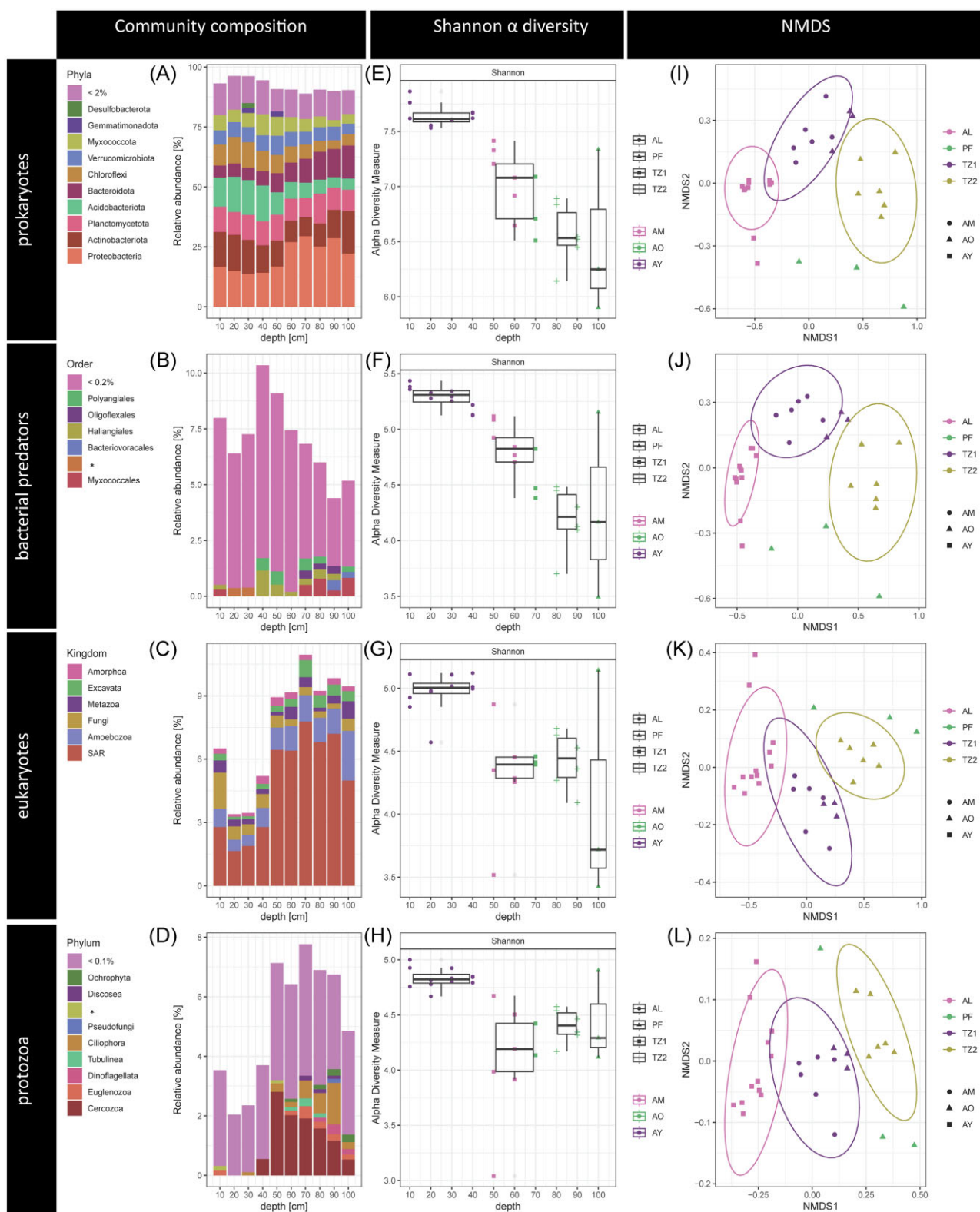


Figure 3. All figures are given for subsets of the total community with prokaryotes, bacterial predators, eukaryotes, and protozoan rRNA. Bar plots indicating the relative mean abundance per depth for varying taxonomic orders; * indicates undefined taxonomic levels/incertae sedis. Shannon alpha diversity is given as boxplots with whiskers indicating standard deviation across triplicates. Nonmetric multidimensional scaling (NMDS, middle column) ordination plots performed on rRNA contig abundances per sample. Colours indicate different layers and shape different age horizons. Environmental parameters here are given as layer (active layer: AL, transition zone 1: TZ1 and 2: TZ2, and permafrost: PF) as well as age with young soils (AY), 2634–3770-year-old soil of medium age (AM), and old material (AO) of up to 22 100–26 500 years ago.

reads and decreased with depth. Microeukaryotes made up 90.4% of all eukaryotic rRNA contigs and consisted of 58% of the supergroup Stramenopiles-Alveolata-Rhizaria (SAR) rRNA contigs ($4.7\% \pm 0.1\%$ of total counts), its relative abundance increasing in the transition zones (Fig. 3C). SAR rRNA contigs, together with Amoebozoa and several Amorphea rRNA contigs made up protozoan microbiome predators.

Microbiome predatory community

Out of the 744 rRNA contigs assigned to predatory taxa, 497 were bacterial and 247 eukaryotic. The total proportion of predatory taxa within the total community ranged from 7.9% to 26.3%, peaking at 40–50 cm depth within the permafrost soil first thawed after the collapse. The ratio of protozoa to bacterial predators indicated a higher abundance of protozoa with depth, while predatory bacteria dominated especially within the active layer (Supplementary Table 3). Predator relative abundance significantly correlated with the total (protozoa: $F_{\text{Model}} = 5.49$, $R^2 = 0.407$, $P = .006$; bacterial predators $F_{\text{Model}} = 3.16$, $R^2 = 0.283$, $P = .026$) and each subcommunity (Table 2). Several nonpredatory prokaryote abundances decreased in depths where predator abundance increased. Hence, we selected both taxa depleted and enriched in the TZ as potential prey and found that a similar significance level and effect size for Alphaproteobacteria, Actinobacteria, and Bacteroidota as for the total nonpredatory community (Supplementary Table 2). No prey groups could be confirmed statistically, neither by testing of selected taxa (Supplementary Table 2), nor by network-based identification of co-occurrence of predators and prokaryotes, as performed with SPIEC-EASI (Supplementary Fig. 4).

Bacterial predators

Bacterial predatory rRNA contigs constituted on average $6.5\% \pm 0.1\%$ of the total microbial community. They included the former proteobacterial order, now recognised as independent bacterial phyla: Myxococcota, and in lower abundances Bdellovibrionota, as well as three gammaproteobacterial *Lysobacter* and three Vampirotvibrionales rRNA contigs (Fig. 3B; Supplementary Table 3). With 48.6% of all predator counts, Myxococcota was the overall most abundant predator with 343 rRNA contigs ($6.0\% \pm 0.1\%$ of total counts).

Protozoa

Protozoa included 247 rRNA contigs ($5.0\% \pm 0.1\%$ of total counts), mostly represented by rRNA contigs from the SAR clade. Cercozoa ($1.7\% \pm 0.0\%$) and Ciliophora ($1.7\% \pm 0.2\%$) dominated the protozoan community (Fig. 3D; Supplementary Table 3). They were abundant in both transition zones and reached a maximum abundance at 60–70 cm depth (Fig. 3A), the deepest thaw level recorded in 2019 (Fig. 1D). Amoebozoa were less abundant ($0.7\% \pm 0.0\%$) and mainly represented in the active layer and TZ1. *Lobosa* rRNA contigs were most abundant at 40–60 cm within the first thaw horizon TZ1 (Fig. 2D).

Diversity and drivers of variance within community composition

Taxonomic richness on average reached 5836 ± 317 , while Shannon (S) alpha diversity was on average 7.17 ± 0.53 for the total community (Supplementary Table 1). Both diversity indices indicate overall high alpha diversity in the active layer and a slight decrease with depth (Fig. 3E–H).

The overall community composition most significantly differed with depth (PERMANOVA, $F_{\text{Model}} = 6.81$, $R^2 = 0.460$, $P =$

$.001$), layer (PERMANOVA, $F_{\text{Model}} = 6.42$, $R^2 = 0.445$, $P = .003$), and SOM (PERMANOVA, $F_{\text{Model}} = 4.77$, $R^2 = 0.373$, $P = .003$). Furthermore, H₂O (PERMANOVA, $F_{\text{Model}} = 5.23$, $R^2 = 0.395$, $P = .005$) explained a significant proportion of the variation of the total community. Age correlated with all community variances except for bacterial predators, while pH was not significant for prokaryotic but for eukaryotic community variance (Table 2). For both, the total and each subcommunity except bacterial predators, only active layer and permafrost differed significantly from each other, while no other layers did (Tukey HSD test, adj. $P < .05$).

Especially, H₂O, SOM, and layer significantly correlated (ANOVA, $P < .005$). Variance partitioning indicated that thaw-related edaphic properties (layer, soil moisture), predation (bacterial and eukaryotic predator abundance), and long-term soil characteristic (SOM, pH, age) together explained 51.5% of the variance in beta diversity of the whole community, with the largest partition contributed to thaw (34.8%; Fig. 2). The ordination of subset communities indicated a gradual transition from active layer to TZ1 and TZ2 samples (Fig. 3I–L), while permafrost samples were visually apart as confirmed by PERMANOVA results.

Discussion

In this study, we aimed to elucidate the response of the total active permafrost microbial community in up to 26500-year-old material under in situ abrupt thaw conditions. Within the Arctic, particularly Greenland and abrupt erosions sites are highly understudied (Malard and Pearce 2018, Metcalfe et al. 2018). Here, we performed the first total RNA metatranscriptomic analysis of the entire active microbial community in such an environment.

We successfully sequenced soil samples down to depths of ancient, intact permafrost and found increased microbial activity at recently thawed layers and changing abundances of microeukaryotes, including bacteria-feeding protozoa. Using metatranscriptomics, we were able to capture the increased presence and putative activity of fast-growing taxa upon thaw. To understand which taxa are responsible for the increased activity upon thaw, we here analysed the total community for prokaryotic and eukaryotic taxa associated with a potentially copiotrophic as well as predatory lifestyle. In our study, the overall alpha diversity compared to former metatranscriptomic research on permafrost microbiomes (Tveit et al. 2015), or even higher (Hultman et al. 2015, Schostag et al. 2019). The deepest thaw horizon indicated overall fewer and less active taxa than expected, compared to former amplicon-based findings (Scheel et al. 2022), although a few fast-growing taxa (Burkholderiales, Sphingobacteriales, and Myxococcota) dominated these depths.

Community composition in eroding permafrost

The use of total RNA sequencing enabled the description of the entire soil community with full-length rRNA analysis, including prokaryotic and eukaryotic microbial taxa. The few metatranscriptomic studies from permafrost environments confirmed similar relative abundances of all domains (Hultman et al. 2015, Tveit et al. 2015, Schostag et al. 2019). In our study, most prokaryotes were represented by proteobacterial taxa, which were formerly reviewed as major taxon of both intact permafrost and active layer microbial communities (Jansson and Tas 2014, Malard and Pearce 2018). While these studies have detected eukaryotic taxa, we found higher abundances than observed previously (Tveit et al. 2015). The overall low fungal abundances in our study could

Table 2. Results of permutational multivariate analysis on the mean Bray–Curtis dissimilarities per depths between total community, prokaryotic, bacterial predators (bacpred), microeukaryotic, and protozoan rRNA contigs.

Env. parameter	Total			Prokaryotes			Bacpred			Microeukaryotes			Protozoa		
	F.Model	R ²		F.Model	R ²		F.Model	R ²		F.Model	R ²		F.Model	R ²	
Depth	6.81	0.460	***	6.84	0.461	***	6.44	0.446	***	5.98	0.428	***	6.88	0.462	***
Age	5.11	0.288	*	2.89	0.265	*	2.71	0.253		2.91	0.266	*	3.68	0.315	*
Layer	6.42	0.445	***	5.73	0.417	***	5.92	0.425	**	4.12	0.340	**	4.98	0.384	***
AL-PF			*			*			NS			**			*
SOM	4.77	0.373	***	4.76	0.373	***	4.89	0.379	***	3.68	0.315	**	4.16	0.342	**
H ₂ O	5.23	0.395	**	5.22	0.395	**	5.42	0.404	**	4.32	0.351	**	5.07	0.388	***
pH	2.54	0.241	NS	2.53	0.240	NS	2.62	0.246	NS	2.42	0.233	*	2.81	0.260	*
Bacpred ^a	3.16	0.283	*	3.20	0.286	*	-	-	-	2.83	0.261	*	2.83	0.261	*
Protozoa ^b	5.49	0.407	**	3.42	0.404	**	5.38	0.402	***	4.64	0.367	**	-	-	-

These were tested against the depth, age, layer, SOM, and moisture (H₂O), and pH. P-values < .05 were considered significant with *P < .05, **P < .01, and ***P < .005. Nonsignificant (NS) categories and pair-wise contrasts in age or layer were removed. Extended data on predatory and potential prey abundances can be found in [Supplementary Table 2](#). ^aThe effect of bacpred abundance was tested on nonpredatory prokaryotes; ^bThe effect of protozoan abundance was tested on nonpredatory eukaryotes in order to prevent artifacts.

relate to a rapid decrease of fungi upon thaw (Hultman et al. 2015).

Thaw and other abiotic drivers

In this study, abiotic factors, such as the soil depth and layer, SOM content, moisture, and age, as well as biotic processes, such as predation significantly correlated with the overall microbial community. Variance partitioning showed that even a combination of short-, long-term, and predatory effects could only explain half of variance in community composition. Hence, we propose further studies to include the analysis of soil nutrients, including N and phosphorus compounds, and temperature logging before sampling.

The strong correlation between soil moisture and the microbial community can be an artefact as the high soil moisture coincide with the active layer. Here, precipitation is likely the main source of soil moisture, while changes in soil moisture at deeper depths might be most impacted by the melting of the former ice lens. Only the active layer and permafrost communities significantly differed from each other. After the former dispersal-limiting ice lens melted, a slow and gradual migration from the active to deeper thawed layers might be expected (Bottos et al. 2018). Such events could explain why no significant differences in rRNA community composition were found between the two thawed depths. The counts per contig ratios and thus potential activity were lowest in the active layer and maximum in the transition zone samples, where the most abundant contigs were annotated largely annotated as Burkholderiales ([Supplementary Fig. 3](#)).

Copiotrophs in thawing permafrost soil

Within the prokaryotic community, the most abundant taxa dominated within the recently thawed permafrost material ([Supplementary Fig. 3](#)), in agreement with a former amplicon-based study in this site (Scheel et al. 2022). Overall, proteobacterial rRNA contigs were the most abundant and encompassed the most phylogenetically diverse groups. We found that Burkholderiales was the most abundant order, with accordance former DNA-based findings from Arctic soils (Malard and Pearce 2018, Scheel et al. 2022). Gammaproteobacteria include many copiotrophic representatives, which were formerly observed to quickly respond to freshly available resources upon permafrost thaw (Hurst 2019, Schostag et al. 2019). Especially, short-term stressors were seen to

trigger a dominance of soil copiotrophs (Koyama et al. 2014, Bang-Andreasen et al. 2020), which might explain why these also had the biggest partition in explaining variance as opposed to long-term and biotic soil properties (Fig. 2).

Burkholderiales peaked in abundance throughout the thawed permafrost depths. Especially Comamonadaceae, a family that consists of many copiotrophic spore-formers, rapidly respond to fresh input of labile nutrients (Fierer et al. 2007, Ho et al. 2017). This suggests that these mineral weathering Burkholderiales (Naylor et al. 2022) might be readily responsive to thawing and hence bioavailable permafrost carbon. The thawing of permafrost soils poses a large potential liberation of organic and inorganic N into the arctic subsoils for microbial uptake (Keuper et al. 2012, Voigt et al. 2017, 2020, Marushchak et al. 2021, Wegner et al. 2022). Here, we show a large potential for rapid N-cycling when permafrost thaws. Notably, most contigs with maximum relative abundances at 70 cm, were the abundant Gallionellaceae (Burkholderiales, Gammaproteobacteria) (Hallbeck and Pedersen 2014), which contain nitrate-dependent iron-oxidising taxa (He et al. 2016). This family was previously found in intact ancient permafrost (Alawi et al. 2007, Müller et al. 2018, Scheel et al. 2022).

Similarly, the particularly active Bacteroidota order Sphingobacteriales dominated recently thawed permafrost, as found during thaw before (Müller et al. 2018). The relative abundance of Bacteroidota increased with depth, potentially indicating that some of its members are more active in permafrost. Yet, high abundances of several copiotrophic order might be an RNA sequencing artefact, where even inactive cells, such as cysts and spores, might contain enough ribosomes so that the contained RNA depicts a corresponding potential activity. This stands against an idea of migrating or being washed down from the active layer, as overall abundances in the active layer were low. In our study site, Sphingobacteriales had the highest relative abundance within the total amplicon-based community composition (Scheel et al. 2022). They then constituted more than half of all counts between 70 and 90 cm depth in 2020. This stands in contrast with very low 16S rRNA-based abundances 1 year earlier (Scheel et al. 2022), which suggests that Sphingobacteriales abundances found in this study reflect a recent increase in response to thaw. Several Bacteroidota taxa were documented as initial metabolisers of labile carbon (Fierer et al. 2007, Ho et al. 2017, Stone et al. 2023). Especially at the upper permafrost limit (Müller et al. 2018, Tripathi

et al. 2018), Bacteroidota abundances also increased in response to thaw (Frank-Fahle et al. 2014, Coolen and Orsi 2015, Deng et al. 2015, Burkert et al. 2019).

Predation as and biotic driver in response to thaw

The abundance of both bacterial and protozoan predators correlated with each subcommunity. This supports our findings that indicate that predator abundance was important to the system as a biological control of increased microbial activity but might not have acted as the main driver of taxonomic changes across depths. In a former study investigating the impact of nematodes and protozoa on different bacterial lifestyles under nutrient addition showed that oligotrophic taxa often served as prey, the overall bacterial growth being more impacted by nutrient availability than predation (Zelenev et al. 2006).

Potential prey and predation interactions

Several microorganisms have protective measures against predation (Trap et al. 2016). Some protozoa taxa grew less successfully on gram-positive bacteria (Trap et al. 2016), such as Actinobacteriota, which were more abundant in permafrost. This protection might partly be achieved through their formation of filaments, biofilms and colonies, cell size, shape, pigments, and toxins. Here, we noted the decrease of Actinobacteria in the first transition zone, where predators were abundant. Yet, protozoan abundance did not correlate with Actinobacteria abundance more strongly than with other taxa. In contrast, gram-negative bacteria are suitable prey especially to Myxobacteria (the phyla Myxococcota and Bdellovibrionota) and protists (Trap et al. 2016). Hence, the increase of activity of gram-negative Proteobacteria in the thaw zone led us to the idea that potentially fast-growing prey could support a consecutive predator succession. Myxobacteria were earlier found to feed select on gram-negative bacteria, while protozoa showed less selective feeding (Zhang and Lueders 2017). This might be reflected in the overall stronger correlation of protozoan abundance with the total and subcommunities. Although species specific feeding had been found among protozoa (Rønn et al. 2001, Pedersen et al. 2011), interkingdom interactions based on a network (Supplementary Fig. 4) indicated more interactions among nonpredatory taxa than among predatory and their potential prey. This could indicate a higher importance of symbiotic processes or competition, as well as other environmental processes that override the potential impact of predation in our system (Fig. 2).

Bacterial predators dominate shallower thaw layers

Bacterial predators and particularly Myxococcota play key roles in microbial food webs, as recently demonstrated (Dai et al. 2021, Petters et al. 2021). Former studies have shown Myxococcota to be abundant in active layer samples (Inglese et al. 2018, Malard and Pearce 2018, Romanowicz and Kling 2022), especially also in this site (Scheel et al. 2022). Within the active layer, seasonally increased prokaryotic biomass could support higher predator abundances. We hypothesise that the spore-containing fruiting bodies in Myxococcota (Huntley et al. 2011) might resist the winter freeze-off, while the freeze-induced mortality of prey taxa might supply the growth substrate for Myxococcota in spring (Bang-Andreasen et al. 2020). Bdellovibrionota abundances were low. These flagellated bacteria have a smaller prey range and potentially might thrive were competition with Myxococcota is lower (Petters et al. 2021).

Protozoa as active predators present in permafrost soils

Protozoa of this permafrost study were dominated by Ciliophora, Cercozoa, and Amoebozoa in agreement with former studies (Shatilovich et al. 2009, Schostag et al. 2019). Protozoa were most abundant in both thawed permafrost layers, making them more abundant predators than Myxobacteria, which, in turn, dominated the active and shallow first thaw layer (Fig. 3B and D). The smaller Ciliophora and Cercozoa might have responded quickly to permafrost thaw reaching maximum abundances at both thaw horizons. One potential explanation for the high abundance of protozoa in freshly thawed permafrost could be their mobility in water-saturated soils after the ice lens melted. Further, cyst- and resting-stage-forming protist taxa can respond quickly to environmental changes (Rønn et al. 2012).

Interestingly, among the few permafrost metatranscriptomic studies performed, increases in relative abundance of protozoan taxa with increasing temperature were not mentioned (Schostag et al. 2019), while an increase of Cercozoa was observed (Tveit et al. 2015) which could explain their original (2015). Although our relative abundances of Cercozoa matches those of former studies (Geisen et al. 2015, Tveit et al. 2015, Schostag et al. 2019), we expected higher overall abundances at the most recently available thaw horizon at 90 cm. Due to their relatively smaller size, Cercozoa reproduce faster than larger microeukaryotes (Rønn et al. 2012). Furthermore, members of this group have been shown to respond to permafrost thaw within days (Schostag et al. 2019), as well as to temperature increases in Arctic peat (Tveit et al. 2015). Ciliates and Amoeba respond very rapidly to changes in soil moisture (Coleman and Wall 2015) and temperature (Schostag et al. 2019) and have even been found in ancient Siberian permafrost (Shatilovich et al. 2009). Although some studies reported living nematodes and Amoebozoa in ancient permafrost (Shmakova and Rivkina 2015, Shatilovich et al. 2023), their response to permafrost thaw remains unclear.

Our findings suggest that eukaryotic predators dominate during the initial stages of the thaw-triggered microbial activity, while during later stages of thaw increased relative abundance of the less mobile bacterial predators occurred. Furthermore, protozoans might also benefit from the unselective feeding mechanisms in contrast to the more selective Myxobacteria (Zhang and Lueders 2017). This potentially explains why we observed changes in distribution with depth and significant impact of protozoan, but not myxobacterial abundance on potential prey taxa.

Microbial activity during thaw and potential coalescence

Predation bears the obvious potential to reduce and hence control microbial population growth, but also has been found to lead to higher yields in artificial diverse incubation communities. This effect might be due to reduced competition among prey taxa (Saleem et al. 2012), through that keeping populations in growth phase (Mattison and Harayama 2001), as well as potentially leaching nutrients from prey cell lysis. This could explain, why predator abundance correlated with every subcommunity, likely indicating indirect rather than direct predation effects on the whole community. We noted that both prokaryotic and eukaryotic taxa were present among the most active contigs in the thawed layers. Thus, our findings of higher RNA:DNA ratios at the freshly thawed 50 and 80 cm depths indicated higher ribosomal relative abundance of both domains at these depths (Table 1; Supplementary Fig. 1).

The difference in the composition of the active microbial community between shallow and deeper thawed permafrost lay-

ers could result from multiple ecological processes simultaneously impacting the microbial community composition. For example, (1) a steady migration of microorganisms from the active layer to the thawed layers, compared to the below permafrost layer, and (2) rapidly increased microbial activity in recently thawed, former permafrost layers. Ecological responses of soil microbiomes to environmental stress are nonlinear and complex, arising from simultaneous stochastic and deterministic environmental selection (Doherty et al. 2020, Ernakovich et al. 2022).

The peaking activity in ancient, former frozen permafrost, could stem from endemic spores and resting stages. Situated by the Zackenberg river, the oldest sand and rubble deposits (AO) indicate a fluvial origin, potentially as part of the Zackenberg river or glacial meltwater delta into the fjord roughly 30 000 years ago (Gilbert et al. 2017), while younger material could resemble a former pond, that later became overgrown (AM). Arctic fluvial habitats showed higher abundances of Bacteroidota and Proteobacteria in a summer glacial river, but also the Arctic Lake Hazen sediments (Cavaco et al. 2019) and subglacial habitats (Achberger et al. 2017), which could explain their origin even in our samples of ancient and still intact permafrost. Simultaneously, dominance of Bacteroidota was also found in permafrost metatranscriptomes during thaw (Hultman et al. 2015, Schostag et al. 2019).

In contrast to the idea of increased activity in former cold-adapted taxa, earlier findings showed the potential for migration of taxa from the active layer to thawing permafrost (Rillig et al. 2015). In their previous incubation study, Monteux and colleagues found an increase of Bacteroidota abundance upon thaw, after inoculating permafrost with grassland soil (Monteux et al. 2020). Both the processes of a thaw control as well as implantation of temperate soil have resulted in elevated nitrification and CO₂ emissions (Monteux et al. 2020). This highlights the importance of understanding community dynamics in response to thaw. This process was also observed upon transplantation of grassland soil microbiomes onto permafrost (Monteux et al. 2020). Such mixing conditions occurs naturally during cryoturbation of permafrost, such as during a collapse (Gittel et al. 2014, Schneckner et al. 2014), active layer detachments (Inglese et al. 2018), or increased root growth (Monteux et al. 2020). Although we could not statistically separate the potential effects of isolated permafrost thaw and coalescence with the active layer community, they might supply a higher functional diversity to overcome this limitation and hence enhance C and N from thawed permafrost.

Conclusion

We have described the total prokaryotic and microeukaryotic community composition abrupt permafrost erosion stress in High Arctic Greenland based on total RNA sequencing of *in situ* samples. The composition of the total community correlated both with short- and long-term soil properties, including thaw layer, soil moisture, and organic matter content. The high microbial activity we found within freshly thawed permafrost, as indicated by large increases in the RNA:DNA ratio, coincided with an increase of copiotrophic taxa, included representation of Sphingobacteriales and Burkholderiales. This potentially rapid development of microbial biomass at thawed depths also formed the base of a solid bacteria-feeding community dominated by protozoa in recently thawed soil and bacterial predators just below the historical active layer boundary. We found that predation, addi-

tionally to abiotic processes, correlated with changes in the active microbial community composition and highlights the importance of trophic interactions as ecological response to permafrost collapse.

Author contributions

Maria Scheel (Conceptualization, Data curation, Formal analysis, Investigation, Methodology, Project administration, Resources, Software, Visualization, Writing – original draft, Writing – review & editing), Athanasios Zervas (Data curation, Investigation, Methodology, Software, Supervision, Writing – review & editing), Ruud Rijckers (Formal analysis, Methodology, Software, Validation, Writing – review & editing), Alexander Tødsdal Tveit (Conceptualization, Investigation, Methodology, Validation, Writing – review & editing), Flemming Ekelund (Conceptualization, Validation, Writing – review & editing), Francisco Campuzano Jiménez (Formal analysis, Software, Visualization, Writing – review & editing), Torben Røjle Christensen (Data curation, Funding acquisition, Project administration, Resources, Supervision, Writing – review & editing), and Carsten Suhr Jacobsen (Conceptualization, Funding acquisition, Methodology, Project administration, Resources, Supervision, Writing – review & editing)

Acknowledgements

We thank the Zackenberg Research Station staff, the Greenland Ecosystem Monitoring programme facilities, and its field assistants for smooth sample handling of the sampling and samples.

Supplementary data

Supplementary data is available at *FEMSEC Journal* online.

Conflict of interest: None declared.

Funding

This work was supported by the Faculty of Science and Technology, Aarhus University, and the Greenland Ecosystem Monitoring programme.

Data availability

The raw sequence data of this study were deposited in the NCBI Sequence Read Archive and can be accessed through accession number PRJNA939404.

References

- Abbott BW, Brown M, Carey JC et al. We must stop fossil fuel emissions to protect permafrost ecosystems. *Front Environ Sci* 2022;**10**:889428. <https://doi.org/10.3389/fenvs.2022.889428>.
- Achberger AM, Michaud AB, Vick-Majors TJ et al. Microbiology of subglacial environments. In: Margesin R (eds.), *Psychrophiles: From Biodiversity to Biotechnology*. Cham: Springer, 2017. https://doi.org/10.1007/978-3-319-57057-0_5
- Alawi M, Lipski A, Sanders T et al. Cultivation of a novel cold-adapted nitrite oxidizing betaproteobacterium from the Siberian Arctic. *ISME J* 2007;**1**:256–64.
- Allison SD, Martiny JBH. Resistance, resilience, and redundancy in microbial communities. *Proc Natl Acad Sci USA* 2008;**105**:11512–9.

- AMAP. Arctic Climate Change Update 2021: Key Trends and Impacts. Summary for Policy-makers. Arctic Monitoring and Assessment Programme (AMAP), Tromsø, Norway, p. viii+148, 2021.
- Anwar MZ, Lanzen A, Bang-Andreasen T et al. To assemble or not to resemble—a validated comparative metatranscriptomics workflow (CoMW). *Gigascience* 2019;**8**:giz096.
- Bang-Andreasen T, Anwar MZ, Lanzen A et al. Total RNA sequencing reveals multilevel microbial community changes and functional responses to wood ash application in agricultural and forest soil. *FEMS Microbiol Ecol* 2020;**96**:fiaa016.
- Bardgett RD, Caruso T. Soil microbial community responses to climate extremes: resistance, resilience and transitions to alternative states. *Philos Trans R Soc Lond B Biol Sci* 2020;**375**:20190112.
- Bardgett RD, van der Putten WH. Belowground biodiversity and ecosystem functioning. *Nature* 2014;**515**:505–11.
- Bonkowski M. Protozoa and plant growth: the microbial loop in soil revisited. *New Phytol* 2004;**162**:617–31.
- Bottos EM, Kennedy DW, Romero EB et al. Dispersal limitation and thermodynamic constraints govern spatial structure of permafrost microbial communities. *FEMS Microbiol Ecol* 2018;**94**:fy110.
- Burkert A, Douglas TA, Waldrop MP et al. Changes in the active, dead, and dormant microbial community structure across a pleistocene permafrost chronosequence. *Appl Environ Microbiol* 2019;**85**:e02646–18.
- Campuzano Jiménez F. AU-ENVS-Bioinformatics/TotalRNA-Snakemake: v1.1.1 (v1.0.1). Zenodo. 2023. <https://doi.org/10.5281/zenodo.7656004>.
- Cavaco MA, St Louis VL, Engel K et al. Freshwater microbial community diversity in a rapidly changing High Arctic watershed. *FEMS Microbiol Ecol* 2019;**95**:fiz161.
- Christensen TR, Lund M, Skov K et al. Multiple ecosystem effects of extreme weather events in the Arctic. *Ecosystems* 2020;**24**:122–36.
- Christiansen HH, Sigsgaard C, Humlum O et al. Permafrost and periglacial geomorphology at Zackenberg. *Adv Ecol Res* 2008;**40**:151–74.
- Coleman DC, Wall DH. Soil fauna: occurrence, biodiversity and roles in ecosystem function. *Soil Microbiol Ecol Biochem* 2015;**4**:111–49.
- Coolen MJ, Orsi WD. The transcriptional response of microbial communities in thawing Alaskan permafrost soils. *Front Microbiol* 2015;**6**:197.
- Dai W, Wang N, Wang W et al. Community profile and drivers of predatory myxobacteria under different compost manures. *Microorganisms* 2021;**9**:2193.
- Deng J, Gu Y, Zhang J et al. Shifts of tundra bacterial and archaeal communities along a permafrost thaw gradient in Alaska. *Mol Ecol* 2015;**24**:222–34.
- Doherty SJ, Barbato RA, Grandy AS et al. The transition from stochastic to deterministic bacterial community assembly during permafrost thaw succession. *Front Microbiol* 2020;**11**:596589.
- Elberling B, Tamstorf MP, Michelsen A et al. Soil and plant community-characteristics and dynamics at Zackenberg. *Adv Ecol Res* 2008;**40**:223–48.
- Ernakovich JG, Barbato RA, Rich VI et al. Microbiome assembly in thawing permafrost and its feedbacks to climate. *Glob Change Biol* 2022;**28**:5007–26.
- Fierer N, Bradford MA, Jackson RB. Toward an ecological classification of soil bacteria. *Ecology* 2007;**88**:1354–64.
- Frank-Fahle BA, Yergeau E, Greer CW et al. Microbial functional potential and community composition in permafrost-affected soils of the NW Canadian Arctic. *PLoS One* 2014;**9**:e84761.
- Geisen S, Hu S, Dela Cruz TEE et al. Protists as catalyzers of microbial litter breakdown and carbon cycling at different temperature regimes. *ISME J* 2021;**15**:618–21.
- Geisen S, Mitchell EAD, Adl S et al. Soil protists: a fertile frontier in soil biology research. *FEMS Microbiol Rev* 2018;**42**:293–323.
- Geisen S, Tveit AT, Clark IM et al. Metatranscriptomic census of active protists in soils. *ISME J* 2015;**9**:2178–90.
- Gilbert GL, Cable S, Thiel C et al. Cryostratigraphy, sedimentology, and the late Quaternary evolution of the Zackenberg River delta, northeast Greenland. *The Cryosphere* 2017;**11**:1265–82.
- Gittel A, Barta J, Kohoutova I et al. Distinct microbial communities associated with buried soils in the Siberian tundra. *ISME J* 2014;**8**:841–53.
- Guillou L, Bachar D, Audic S et al. The Protist Ribosomal Reference database (PR2): a catalog of unicellular eukaryote small subunit rRNA sequences with curated taxonomy. *Nucleic Acids Res* 2013;**41**:D597–604. <https://doi.org/10.1093/nar/gks1160>.
- Hallbeck L, Pedersen K. The family Gallionellaceae. In: Rosenberg E, DeLong EF, Lory S, Stackebrandt E, Thompson F (eds.), *The Prokaryotes*. Berlin, Heidelberg: Springer, 2014. https://doi.org/10.1007/978-3-642-30197-1_398.
- Harder CB, Ronn R, Brejnrod A et al. Local diversity of heathland Cercozoa explored by in-depth sequencing. *ISME J* 2016;**10**:2488–97.
- He S, Tominski C, Kappler A et al. Metagenomic analyses of the autotrophic Fe(II)-oxidizing, nitrate-reducing enrichment culture KS. *Appl Environ Microbiol* 2016;**82**:2656–68.
- Ho A, Di Lonardo DP, Bodelier PLE. Revisiting life strategy concepts in environmental microbial ecology. *FEMS Microbiol Ecol* 2017;**93**:fix006. <https://doi.org/10.1093/femsec/fix006>.
- Hugelius G, Strauss J, Zubrzycki S et al. Estimated stocks of circumpolar permafrost carbon with quantified uncertainty ranges and identified data gaps. *Biogeosciences* 2014;**11**:6573–93.
- Hultman J, Waldrop MP, Mackelprang R et al. Multi-omics of permafrost, active layer and thermokarst bog soil microbiomes. *Nature* 2015;**521**:208–12.
- Huntley S, Hamann N, Wegener-Feldbrugge S et al. Comparative genomic analysis of fruiting body formation in Myxococcales. *Mol Biol Evol* 2011;**28**:1083–97.
- Hurst CJ. *Understanding Terrestrial Microbial Communities*. Cham: Springer, 2019.
- Inglese CN, Christiansen CT, Lamhonwah D et al. Examination of soil microbial communities after permafrost thaw subsequent to an active layer detachment in the high Arctic. *Arct Antarct Alp Res* 2018;**49**:455–72.
- IPCC. *Climate Change 2021: the Physical Science Basis. Contribution of Working Group I to the Sixth Assessment Report of the Intergovernmental Panel on Climate Change*. Cambridge, UK and New York, NY: Cambridge University Press, 2021, 2391. <https://doi.org/10.1017/9781009157896>.
- Jansson JK, Tas N. The microbial ecology of permafrost. *Nat Rev Microbiol* 2014;**12**:414–25.
- Keuper F, Bodegom PM, Dorrepaal E et al. A frozen feast: thawing permafrost increases plant-available nitrogen in subarctic peatlands. *Glob Change Biol* 2012;**18**:1998–2007.
- Kopylova E, Noe L, Touzet H. SortMeRNA: fast and accurate filtering of ribosomal RNAs in metatranscriptomic data. *Bioinformatics* 2012;**28**:3211–7.
- Koyama A, Wallenstein MD, Simpson RT et al. Soil bacterial community composition altered by increased nutrient availability in Arctic tundra soils. *Front Microbiol* 2014;**5**:516.
- Kurtz ZD, Müller CL, Miraldi ER et al. Sparse and compositionally robust inference of microbial ecological networks. *PLoS Comput Biol* 2015;**11**:e1004226.

- Langzen A, Jorgensen SL, Huson DH et al. CREST—classification resources for environmental sequence tags. *PLoS One* 2012;**7**:e49334.
- Lennon JT, Jones SE. Microbial seed banks: the ecological and evolutionary implications of dormancy. *Nat Rev Microbiol* 2011;**9**:119–30.
- Levin I, Kromer B. The tropospheric ¹⁴CO₂ level in mid-latitudes of the Northern hemisphere (1959–2003). *Radiocarb* 2016;**46**:1261–72.
- Li H, Durbin R. Fast and accurate short read alignment with Burrows–Wheeler transform. *Bioinformatics* 2009;**25**:1754–60.
- Malard LA, Pearce DA. Microbial diversity and biogeography in Arctic soils. *Environ Microbiol Rep* 2018;**10**:611–25.
- Marushchak ME, Kerttula J, Diakova K et al. Thawing Yedoma permafrost is a neglected nitrous oxide source. *Nat Commun* 2021;**12**:7107.
- Mattison RG, Harayama S. The predatory soil flagellate *Heteromita globosa* stimulates toluene biodegradation by a *Pseudomonas* sp. *FEMS Microbiol Lett* 2001;**194**:39–45.
- McMurdie PJ, Holmes S. phyloseq: an R package for reproducible interactive analysis and graphics of microbiome census data. *PLoS One* 2013;**8**:e61217.
- Metcalfe DB, Hermans TDG, Ahlstrand J et al. Patchy field sampling biases understanding of climate change impacts across the Arctic. *Nat Ecol Evol* 2018;**2**:1443–8.
- Monteux S, Keuper F, Fontaine S et al. Carbon and nitrogen cycling in Yedoma permafrost controlled by microbial functional limitations. *Nat Geosci* 2020;**13**:794–8.
- Monteux S, Weedon JT, Blume-Werry G et al. Long-term in situ permafrost thaw effects on bacterial communities and potential aerobic respiration. *ISME J* 2018;**12**:2129–41.
- Müller O, Bang-Andreasen T, White RA et al. Disentangling the complexity of permafrost soil by using high resolution profiling of microbial community composition, key functions and respiration rates. *Environ Microbiol* 2018;**20**:4328–42.
- Nannipieri P, Ascher J, Ceccherini MT et al. Microbial diversity and soil functions. *Eur J Soil Sci* 2017;**68**:12–26.
- Naylor D, McClure R, Jansson J. Trends in microbial community composition and function by soil depth. *Microorganisms* 2022;**10**:540.
- Oksanen J, Simpson G, Blanchet F et al. vegan: Community Ecology Package. R package version 2.6-4. 2022. <https://CRAN.R-project.org/package=vegan> (17 October 2023, date last accessed).
- Parmentier FW, Christensen TR, Rysgaard S et al. A synthesis of the arctic terrestrial and marine carbon cycles under pressure from a dwindling cryosphere. *Ambio* 2017;**46**:53–69.
- Pedersen AL, Winding A, Altenburger A et al. Protozoan growth rates on secondary-metabolite-producing *Pseudomonas* spp. correlate with high-level protozoan taxonomy. *FEMS Microbiol Lett* 2011;**316**:16–22.
- Petters S, Gross V, Sollinger A et al. The soil microbial food web revisited: predatory myxobacteria as keystone taxa? *ISME J* 2021;**15**:2665–75.
- Quast C, Pruesse E, Yilmaz P et al. The SILVA ribosomal RNA gene database project: improved data processing and web-based tools. *Nucleic Acids Res* 2013;**41**:D590–6.
- R Core Team. R: A Language and Environment for Statistical Computing. Vienna, Austria: R Foundation for Statistical Computing, 2022. <https://www.R-project.org/> (17 October 2023, date last accessed).
- Rantanen M, Karpechko AY, Lipponen A et al. The Arctic has warmed nearly four times faster than the globe since 1979. *Commun Earth Environ* 2022;**3**:168.
- Reimer PJ, Bard E, Bayliss A et al. IntCal13 and Marine13 radiocarbon age calibration curves 0–50 000 years cal BP. *Radiocarb* 2016;**55**:1869–87.
- Rillig MC, Antonovics J, Caruso T et al. Interchange of entire communities: microbial community coalescence. *Trends Ecol Evol* 2015;**30**:470–6.
- Romanowicz KJ, Kling GW. Summer thaw duration is a strong predictor of the soil microbiome and its response to permafrost thaw in Arctic tundra. *Environ Microbiol* 2022;**24**:6220–37.
- Rønn R, Grunert J, Ekelund F. Protozoan response to addition of the bacteria *Mycobacterium chlorophenicum* and *Pseudomonas chlororaphis* to soil microcosms. *Biol Fertil Soils* 2001;**33**:126–31.
- Rønn R, Vestergård M, Ekelund F. Interactions between bacteria, protozoa and nematodes in soil. *Acta Protozool* 2012;**51**:223–35.
- RStudio Team. RStudio: Integrated Development for R. Boston, MA: RStudio, PBC, 2020. <http://www.rstudio.com/>.
- Saleem M, Fetzer I, Dormann CF et al. Predator richness increases the effect of prey diversity on prey yield. *Nat Commun* 2012;**3**:1305.
- Scheel M, Zervas A, Jacobsen CS et al. Microbial community changes in 26 500-year-old thawing permafrost. *Front Microbiol* 2022;**13**:787146.
- Scheller JH, Mastepanov M, Christiansen HH et al. Methane in Zackenberg Valley, NE Greenland: multidecadal growing season fluxes of a high-Arctic tundra. *Biogeosciences* 2021;**18**:6093–114.
- Schnecker J, Wild B, Hofhans F et al. Effects of soil organic matter properties and microbial community composition on enzyme activities in cryoturbated arctic soils. *PLoS One* 2014;**9**:e94076.
- Schostag M, Prieme A, Jacquiod S et al. Bacterial and protozoan dynamics upon thawing and freezing of an active layer permafrost soil. *ISME J* 2019;**13**:1345–59.
- Schostag MD, Albers CN, Jacobsen CS et al. Low turnover of soil bacterial rRNA at Low temperatures. *Front Microbiol* 2020;**11**:962.
- Schuur EAG, Mack MC. Ecological response to permafrost thaw and consequences for local and global ecosystem services. *Annu Rev Ecol Syst* 2018;**49**:279–301.
- Shade A, Peter H, Allison SD et al. Fundamentals of microbial community resistance and resilience. *Front Microbiol* 2012;**3**:417.
- Shatilovich A, Gade VR, Pippel M et al. A novel nematode species from the Siberian permafrost shares adaptive mechanisms for cryptobiotic survival with *C. elegans* dauer larva. *PLoS Genet* 2023;**19**:e1010798.
- Shatilovich AV, Shmakova LA, Mylnikov AP et al. Ancient protozoa isolated from Permafrost. In: Margesin R (ed.), *Permafrost Soils*. Soil Biology, Vol. 16. Berlin, Heidelberg: Springer, 2009.
- Shmakova LA, Rivkina EM. Viable eukaryotes of the phylum amoebozoa from the Arctic permafrost. *Paleontol J* 2015;**49**: 572–7.
- Stone BWG, Dijkstra P, Finley BK et al. Life history strategies among soil bacteria—dichotomy for few, continuum for many. *ISME J* 2023;**17**:611–9.
- Tarnocai C, Canadell JG, Schuur EAG et al. Soil organic carbon pools in the northern circumpolar permafrost region. *Glob Biogeochem Cycles* 2009;**23**:GB2023.
- Thakur MP, Geisen S. Trophic regulations of the soil microbiome. *Trends Microbiol* 2019;**27**:771–80.
- Trap J, Bonkowski M, Plassard C et al. Ecological importance of soil bacterivores for ecosystem functions. *Plant Soil* 2016;**398**:1–24.
- Tripathi BM, Kim M, Kim Y et al. Variations in bacterial and archaeal communities along depth profiles of Alaskan soil cores. *Sci Rep* 2018;**8**:504.
- Turetsky MR, Abbott BW, Jones MC et al. Carbon release through abrupt permafrost thaw. *Nat Geosci* 2020;**13**:138–43.
- Tveit AT, Urich T, Frenzel P et al. Metabolic and trophic interactions modulate methane production by Arctic peat microbiota in response to warming. *Proc Natl Acad Sci USA* 2015;**112**: E2507–16.

- Voigt C, Marushchak M, Abbott BW et al. Nitrous oxide emissions from permafrost-affected soils. *Nat Rev Earth Environ* 2020;**1**: 420–34.
- Voigt C, Marushchak ME, Lamprecht RE et al. Increased nitrous oxide emissions from Arctic peatlands after permafrost thaw. *Proc Natl Acad Sci USA* 2017;**114**:6238–43.
- Wegner R, Fiencke C, Knoblauch C et al. Rapid permafrost thaw removes nitrogen limitation and rises the potential for N₂O emissions. *MDPI* 2022;**3**:608–27.
- Westergaard-Nielsen A, Karami M, Hansen BU et al. Contrasting temperature trends across the ice-free part of Greenland. *Sci Rep* 2018;**8**:1586.
- Westermann S, Elberling B, Højlund Pedersen S et al. Future permafrost conditions along environmental gradients in Zackenberg, Greenland. *The Cryosphere* 2015;**9**:719–35.
- Wilke B-M. Determination of chemical and physical soil properties. In Margesin R, Schinner F (eds.), *Manual for Soil Analysis*, Vol. 5. Berlin-Heidelberg: Springer Verlag, 2005.
- Xue Y, Lanzen A, Jonassen I. Reconstructing ribosomal genes from large scale total RNA meta-transcriptomic data. *Bioinformatics* 2020;**36**:3365–71.
- Zelenev AA, van Bruggen AHC, Leffelaar PA et al. Oscillating dynamics of bacterial populations and their predators in response to fresh organic matter added to soil: The simulation model 'BACWAVE-WEB'. *Soil Biol Biochem* 2006;**38**:1690–1711. <https://doi.org/10.1016/j.soilbio.2005.11.024>.
- Zhang L, Lueders T. Micropredator niche differentiation between bulk soil and rhizosphere of an agricultural soil depends on bacterial prey. *FEMS Microbiol Ecol* 2017;**93**: fix103